

Temporal characteristics of an optical soliton with distributed Raman amplification

Hongjun Zheng, Shanliang Liu, Xin Li, and Zhen Tian

Citation: [Journal of Applied Physics](#) **102**, 103106 (2007); doi: 10.1063/1.2817478

View online: <http://dx.doi.org/10.1063/1.2817478>

View Table of Contents: <http://scitation.aip.org/content/aip/journal/jap/102/10?ver=pdfcov>

Published by the [AIP Publishing](#)

Articles you may be interested in

[Multiple soliton self-frequency shift cancellations in a temporally tailored photonic crystal fiber](#)

Appl. Phys. Lett. **105**, 181113 (2014); 10.1063/1.4901508

[Nonlinear-optical brain anatomy by harmonic-generation and coherent Raman microscopy on a compact femtosecond laser platform](#)

Appl. Phys. Lett. **99**, 231109 (2011); 10.1063/1.3664345

[Transient Raman response and soliton self-frequency shift in tellurite microstructured fiber](#)

J. Appl. Phys. **108**, 123110 (2010); 10.1063/1.3525595

[Multilayered optical data storage using a spatial soliton](#)

Appl. Phys. Lett. **93**, 241103 (2008); 10.1063/1.3050454

[Temporal and noise characteristics of continuous-wave-pumped continuum generation in holey fibers around 1300 nm](#)

Appl. Phys. Lett. **85**, 2706 (2004); 10.1063/1.1801175



Launching in 2016!

The future of applied photonics research is here

AIP | APL
Photonics

Temporal characteristics of an optical soliton with distributed Raman amplification

Hongjun Zheng^{a)}

*Institute of Optical Communication, Liaocheng University, Liaocheng Shandong, 252059, China
and Department of Electronic Science and Technology, Huazhong University of Science
and Technology, Wuhan Hubei, 430074, China*

Shanliang Liu, Xin Li, and Zhen Tian

Institute of Optical Communication, Liaocheng University, Liaocheng Shandong, 252059, China

(Received 31 August 2007; accepted 15 October 2007; published online 27 November 2007)

The effects of distributed Raman amplification (DRA) on temporal characteristics of an optical soliton that are numerically investigated by using the split-step Fourier method are compared with the experimental data measured by employing the second-harmonic generation frequency-resolved optical gating analyzer. It is found that the numerical results are consistent with the experimental data. DRA that can compensate the fiber loss does not change the temporal wave form of the soliton. The soliton width performs a various oscillation with propagation distance when considering the fiber loss and different Raman gain. Compensation of the fiber loss increases with the increase of the Raman pumping power. © 2007 American Institute of Physics. [DOI: 10.1063/1.2817478]

The distributed Raman amplification (DRA), which is based on stimulated Raman scatter, is an important nonlinear process in a fiber. The DRA has been attracting more and more attention in the applications of optical transmission in recent years because it has more advantages of broad gain bandwidth and low amplified spontaneous emission (ASE) noise than those of erbium-doped optical fiber amplifier (EDFA).^{1–15} However, previous research on the optical soliton transmission system with Raman amplification is normally performed by using the autocorrelation technology so that the temporal wave forms and other characteristics of the pulses cannot be exactly determined.^{11–15} The second-harmonic generation frequency-resolved optical gating (SHG-FROG) analyzer can exactly measure temporal wave form, chirp, and other characteristic parameters of the optical pulse.^{16–18} Recently, we completed the experimental research on propagation characteristics of optical soliton with DRA in single mode fibers by employing the SHG-FROG analyzer. In this paper, effects of DRA on the temporal characteristics of an optical soliton that are numerically investigated by the use of the split-step Fourier method are compared with the experimental data.

We measured the temporal wave form and phase curve, temporal full width at half maximum, and other parameters of 10 GHz, 468 mW input soliton at 1550 nm by using the SHG-FROG analyzer. Then we import the experimental data into the MATLAB program designed by us to obtain the expression of the experimental soliton and other parameters by use of curve fitting. Figure 1 shows the temporal wave form and phase curve of the soliton. Solid curves show the experimental data, which are well fitted by

$$U(0, T) = \sec h \left(\frac{T}{T_0} \right) \exp \left(- \frac{iCT^2}{2T_0^2} \right), \quad (1)$$

where $U(0, T)$ is the incident field of the input soliton, T is the time, $T_0 = 1.47/1.763$ ps is the half-width of the soliton, and $C = -0.35$ is linear frequency chirp parameter.

The DRA is backward-pumped by a continuous wave (cw) laser at 1450 nm. Under cw operation, the effective length of DRA is defined by

$$L_{\text{eff}} = [1 - \exp(-\alpha_p L)] / \alpha_p, \quad (2)$$

where α_p is fiber loss coefficient at pump wavelength and L is the propagation distance. We obtain the experimental data $\alpha_p = 0.29$ dB/km at 1450 nm. $L_{\text{eff}} \approx 1/\alpha_p = 1/(0.29 \times 4.343^{-1}) \approx 15$ km for $\alpha_p L \gg 1$. Then we select two fibers in the experiment. A fiber length (9 km) is less than L_{eff} , the mode field diameter of the fiber is 9.07 μm , the dispersion parameter is 15.07 ps/(nm km) at 1550 nm, the dispersion slope is 0.086 ps/(nm² km), and the fiber loss is 0.188 dB/km. Another fiber length (25.284 km) is more than L_{eff} , the mode field diameter is 9.24 μm , the dispersion parameter is 14.97 ps/(nm km) at 1550 nm, the dispersion slope is 0.086 ps/(nm² km), and the fiber loss is 0.182 dB/km. The Raman gain coefficient is defined by

$$\alpha_R = g \exp[-\alpha_p(L - z)], \quad (3)$$

where z is the propagation variable. One can assume that $g = \alpha_s$ because it is considered that DRA can completely compensate the fiber loss at $z = L$. α_s is the fiber loss coefficient at signal wavelength. The soliton propagation equation with DRA can be modified by

$$i \frac{\partial U}{\partial \xi} + \frac{1}{2} \frac{\partial^2 U}{\partial \tau^2} + |U|^2 U = -0.5i(\alpha_s - \alpha'_R)L_D U, \quad (4)$$

where U is the normalized incident field, ξ is the normalized propagation distance, $\tau = T/T_0$ is the normalized time, and

^{a)}Electronic mail: zhj@lcu.edu.cn. Telephone: 86 635 8231235. FAX: 86 635 8238167. Present address: Institute of Optical Communication, Liaocheng University, Liaocheng Shandong, 252059, China.

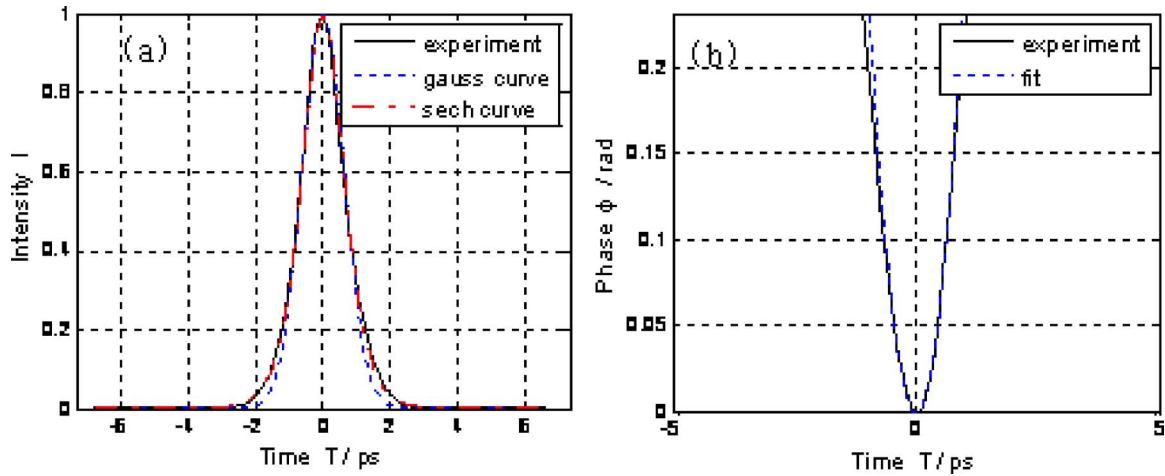


FIG. 1. Temporal wave form (a) and phase curve (b) of the input soliton. Solid curves are experimental data. Dotted and dotted-dashed curves are, respectively, Gaussian and hyperbolic secant curves in Fig. 1(a). The dotted curve is the phase curve of Eq. (1) in Fig. 1(b).

$\alpha'_R = \alpha_s \exp[-\alpha_p(L' - \xi)L_D]$ is the normalized Raman gain coefficient. The effects of DRA on propagation characteristics of the soliton are numerically investigated by use of the split-step Fourier method according to Eq. (4). The input soliton is Eq. (1), propagation distance 9 and 25.284 km are, respectively, normalized to 248.6 and 693.9 dispersion length.

Figure 2 shows that temporal width of the chirped soliton varies with the propagation distance for $\xi=248.6$ by use of the numerical method. The dashed curve is with fiber loss and the solid curve is with fiber loss and DRA. The solid dot and circle are experimental data for the two cases, respectively. The experimental data are measured by use of the SHG-FROG analyzer for $I_p=1$ A (the pumped current of the DRA is 1 A) in Figs. 2–5. It is found that the input soliton with an initial negative chirp periodically broadens with the propagation distance in the lossy fiber, the numerical width 2.675 ps of the output soliton is very consistent with the experimental width 2.712 ps at $\xi=248.6$. The chirped soliton periodically broadens slower than that only with the fiber loss when the fiber loss and DRA are considered. The numerical width 2.01 ps of the output soliton is also very consistent with the experimental width 1.934 ps at $\xi=248.6$ for

the case with the fiber loss and DRA and is in accord with the numerical width 1.804 ps without fiber loss and DRA. It shows that the DRA can completely compensate fiber loss for $L < L_{\text{eff}}$.

Figure 3 shows that the temporal width of the soliton varies with the propagation distance for $\xi=693.9$ by use of the numerical method. It is found that the numerical width of the input soliton periodically broadens to 5.36 ps at $\xi=693.9$, when considering fiber loss, is consistent with the experimental width 5.191 ps. The chirped soliton obviously broadens slower than that considering fiber loss when the fiber loss and DRA are considered. The numerical width 3.158 ps of the output soliton is also consistent with the experimental width 3.075 ps at $\xi=693.9$ for the case with the fiber loss and DRA, is about 1.7 times as wide as the numerical width 1.811 ps only for the case without fiber loss and DRA, and is more than twice the experimental width 1.47 ps of the input soliton. It shows that the DRA can partially compensate fiber loss for $L > L_{\text{eff}}$.

Temporal wave forms of output solitons at $\xi=248.6$ and $\xi=693.9$ are, respectively, shown as Figs. 4 and 5. Figures 4(a) and 5(a) are for the case with fiber loss and Figs. 4(b)

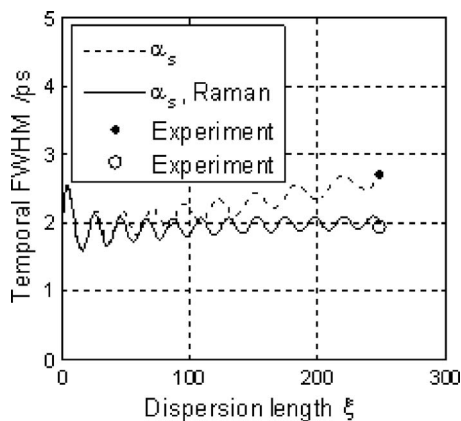


FIG. 2. Variation of temporal width with the propagation distance for $\xi=248.6$. The dashed curve is with fiber loss and the solid curve is with fiber loss and DRA. The solid dot and circle are experimental data for the two cases, respectively.

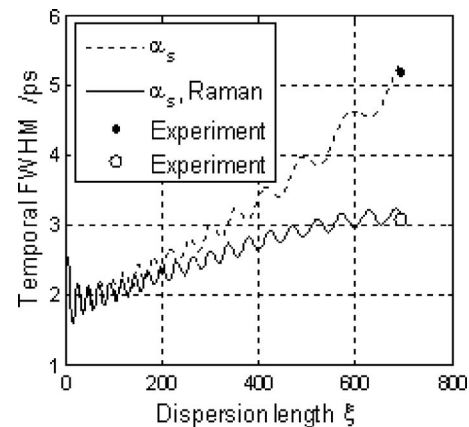


FIG. 3. Variation of temporal width with the propagation distance for $\xi=693.9$. The dashed curve is with fiber loss and the solid curve is with fiber loss and DRA. The solid dot and circle are experimental data for the two cases, respectively.

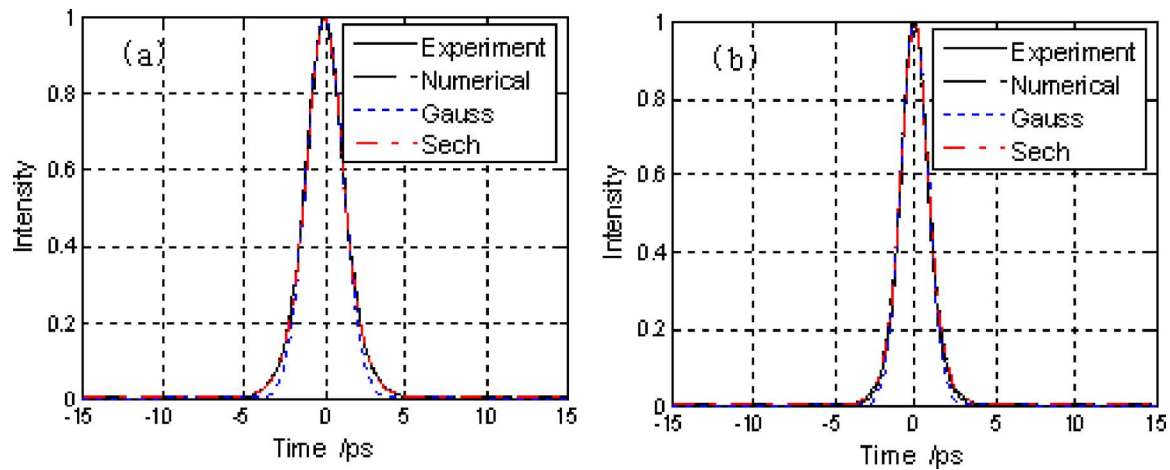


FIG. 4. Temporal wave form of the output soliton at $\xi=248.6$ with fiber loss (a) and with the fiber and DRA (b). The solid curve is the experimental data, the dashed curve is the numerical result, the dotted curve is the Gaussian curve, the dotted-dashed curve is the hyperbolic secant curve.

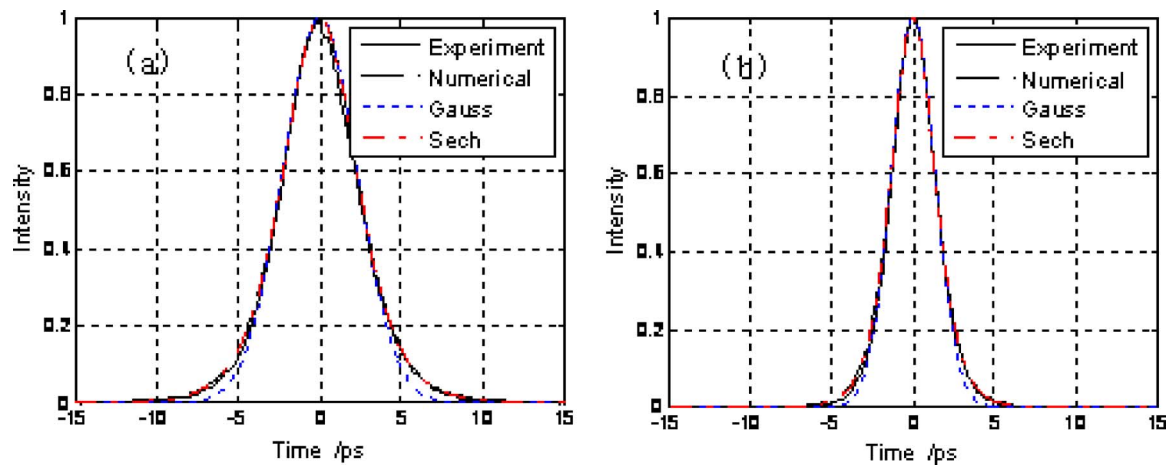


FIG. 5. Temporal wave form of the output soliton at $\xi=693.9$ with fiber loss (a) and with the fiber and DRA (b). The solid curve is the experimental data, the dashed curve is the numerical result, the dotted curve is the Gaussian curve, and the dotted-dashed curve is the hyperbolic secant curve.

and 5(b) are for the case with the fiber loss and DRA. The solid curve shows the experimental wave form, the dashed curve shows the numerical wave form, the dotted curve shows the Gaussian wave form, the dotted-dashed curve shows the hyperbolic secant curve. It can be obtained that the numerical wave form of the output soliton is very consistent with the hyperbolic secant curve and is in accord with the experimental wave form. It shows that the chirped soliton can still maintain a hyperbolic secant curve with fiber loss and DRA and periodically broadens with the propagation distance.

The numerical results are consistent with the experimental data. The DRA can compensate the fiber loss and does not change the temporal wave form of the soliton. The soliton width performs a various oscillation with the propagation distance when considering the fiber loss and different Raman gain. The DRA can completely compensate the fiber loss when the propagation distance is less than the effective fiber length of the DRA and can partially compensate the fiber loss when the propagation distance is more than the effective fiber length. Compensation of the fiber loss increases with the increase of the Raman pumping power.

Project supported by the Research Foundation of Education Department of Shandong Province, China (Grant No. J05C09), the National Natural Science Foundation of China

(Grant No. 60778017), China, and the Research Foundation of Liaocheng University.

- ¹L. F. Mollenauer and K. Smith, *Opt. Lett.* **13**, 675 (1988).
- ²G. F. Levy, *J. Lightwave Technol.* **14**, 72 (1996).
- ³A. G. Okhrimchuk, G. Onishchukov, and F. Lederer, *J. Lightwave Technol.* **19**, 837 (2001).
- ⁴H. N. Ereifej, V. Grigoryan, and G. M. Carter, *Electron. Lett.* **37**, 1538 (2001).
- ⁵E. Pincemin, D. Hamoir, O. Audouin, and S. Wabnitz, *J. Opt. Soc. Am. B* **19**, 973 (2002).
- ⁶S. Chi and S. Wen, *Opt. Lett.* **14**, 84 (1989).
- ⁷S. Wen, T.-Y. Wang, and S. Chi, *IEEE J. Quantum Electron.* **21**, 2066 (1991).
- ⁸G. P. Agrawal, *Opt. Lett.* **16**, 226 (1991).
- ⁹A. A. B. Tio and P. Shum, *Proc. SPIE* **5280**, 676 (2004).
- ¹⁰Y. Li, F. C. Salisbury, Z. Zhu, T. G. Brown, P. S. Westbrook, K. S. Feder, and R. S. Windeler, *Opt. Express* **13**, 998 (2005).
- ¹¹L. F. Mollenauer, R. H. Stolen, and M. N. Islam, *Opt. Lett.* **10**, 229 (1985).
- ¹²A. S. Gouveia-Neto, P. G. J. Wigley, and J. R. Taylor, *Opt. Lett.* **14**, 1122 (1989).
- ¹³K. Iwatsuki, S. Nishi, M. Saruwatari, and K. Nakagawa, *IEEE Photonics Technol. Lett.* **2**, 507 (1990).
- ¹⁴K. Iwatsuki, K.-I. Suzuki, and S. Nishi, *IEEE Photonics Technol. Lett.* **3**, 1074 (1991).
- ¹⁵T. E. Murphy, *IEEE Photonics Technol. Lett.* **14**, 1424 (2002).
- ¹⁶S. Del Burgo, B. C. Thomsen, R. T. Watts, D. A. Reid, and J. Harvey, *IEEE Photonics Technol. Lett.* **14**, 971 (2002).
- ¹⁷S. L. Liu and H. J. Zheng, *Chin. J. Lasers* **33**, 199 (2006) (in Chinese).
- ¹⁸S. L. Liu and H. J. Zheng, *Acta Opt. Sin.* **26**, 1313 (2006) (in Chinese).